We are IntechOpen, the world's leading publisher of Open Access books Built by scientists, for scientists

4,800
Open access books available

122,000
International authors and editors

135M
Downloads

Our authors are among the

154
Countries delivered to

TOP 1%
most cited scientists

12.2%
Contributors from top 500 universities

CLARIVATE ANALYTICS BOOK CITATION INDEX INDEXED

WEB OF SCIENCE™

Selection of our books indexed in the Book Citation Index in Web of Science™ Core Collection (BKCI)

Interested in publishing with us?
Contact book.department@intechopen.com

Numbers displayed above are based on latest data collected.
For more information visit www.intechopen.com

Chapter 9

Vibrations of Cylindrical Shells

Tiejun Yang, Wen L. Li and Lu Dai

Additional information is available at the end of the chapter

http://dx.doi.org/10.5772/51816

1. Introduction

Beams, plates and shells are the most commonly-used structural components in industrial applications. In comparison with beams and plates, shells usually exhibit more complicated dynamic behaviours because the curvature will effectively couple the flexural and in-plane deformations together as manifested in the fact that all three displacement components simultaneously appear in each of the governing differential equations and boundary conditions. Thus it is understandable that the axial constraints can have direct effects on a predominantly radial mode. For instance, it has been shown that the natural frequencies for the circumferential modes of a simply supported shell can be noticeably modified by the constraints applied in the axial direction [1]. Vibrations of shells have been extensively studied for several decades, resulting in numerous shell theories or formulations to account for the various effects associated with deformations or stress components.

Expressions for the natural frequencies and modes shapes can be derived for the classical homogeneous boundary conditions [2-9]. Wave propagation approach was employed by several researchers [10-13] to predict the natural frequencies for finite circular cylindrical shells with different boundary conditions. Because of the complexity and tediousness of the (exact) solution procedures, approximate procedures such as the Rayleigh-Ritz methods or equivalent energy methods have been widely used for solving shell problems [14-18]. In the Rayleigh-Ritz methods, the characteristic functions for a "similar" beam problem are typically used to represent all three displacement components, leading to a characteristic equation in the form of cubic polynomials. Assuming that the circumferential wave length is smaller than the axial wave length, Yu [6] derived a simple formula for calculating the natural frequencies directly from the shell parameters and the frequency parameters for the analogous beam case. Soedel [19] improved and generalized Yu's result by eliminating the short circumferential wave length restriction. However, since the wavenumbers for axial modal function are obtained from beam functions which do not exactly satisfy shell boundary con-

ditions, it is mathematically difficult to access or ensure the accuracy and convergence of such a solution.

The free vibration of shells with elastic supports was studied by Loveday and Rogers [20] using a general analysis procedure originally presented by Warburton [3]. The effect of flexibility in boundary conditions on the natural frequencies of two (lower order) circumferential modes was investigated for a range of restraining stiffness values. The vibrations of circular cylindrical shells with non-uniform boundary constraints were studied by Amabili and Garziera [21] using the artificial spring method in which the modes for the corresponding less-restrained problem were used to expand the displacement solutions. The non-uniform spring stiffness distributions were systematically represented by cosine series and their presence was accounted for in terms of maximum potential energies stored in the springs.

A large number of studies are available in the literature for the vibrations of shells under different boundary conditions or with various complicating features. A comprehensive review of early investigations can be found in Leissa's book [22]. Some recent progresses have been reviewed by Qatu [23]. Regardless of whether an approximate or an exact solution procedure is employed, the corresponding formulations and implementations usually have to be modified or customized for different boundary conditions. This shall not be considered a trivial task in view that there exist 136 different combinations even considering the simplest (homogeneous) boundary conditions. Thus, it is useful to develop a solution method that can be generally applied to a wide range of boundary conditions with no need of modifying solution algorithms and procedures. Mathematically, elastic supports represent a general form of boundary conditions from which all the classical boundary conditions can be readily derived by simply setting each of the spring stiffnesses to either zero or infinity. This chapter will be devoted to developing a general analytical method for solving shell problems involving general elastically restrained ends.

2. Basic equations and solution procedures

Figure 1 shows an elastically restrained circular cylindrical shell of radius R, thickness h and length L. Each of the eight sets of elastic restraints shall be understood as a distributed spring along the circumference. Let u, v, and w denote the displacements in the axial x, circumferential θ and radial r directions, respectively. The equations of the motions for the shell can be written as

$$\begin{aligned} &\frac{\partial N_1}{\partial x}+\frac{\partial N_{12}}{R\partial\theta}=\rho h\frac{\partial^2 u}{\partial t^2} && \text{(a)}\\ &\frac{\partial N_{12}}{\partial x}+\frac{\partial N_2}{R\partial\theta}=\rho h\frac{\partial^2 v}{\partial t^2} && \text{(b)}\\ &\frac{\partial Q_1}{\partial x}+\frac{\partial Q_1}{R\partial\theta}-\frac{N_2}{R}=\rho h\frac{\partial^2 w}{\partial t^2} && \text{(c)} \end{aligned} \tag{1}$$

http://dx.doi.org/10.5772/51816

where ρ is the mass density of the shell material, and N_1, N_{12}, $N_{\circledcirc}$, Q_1 and $Q_{\circledcirc}$ denote the resultant forces acting on the mid-surface.

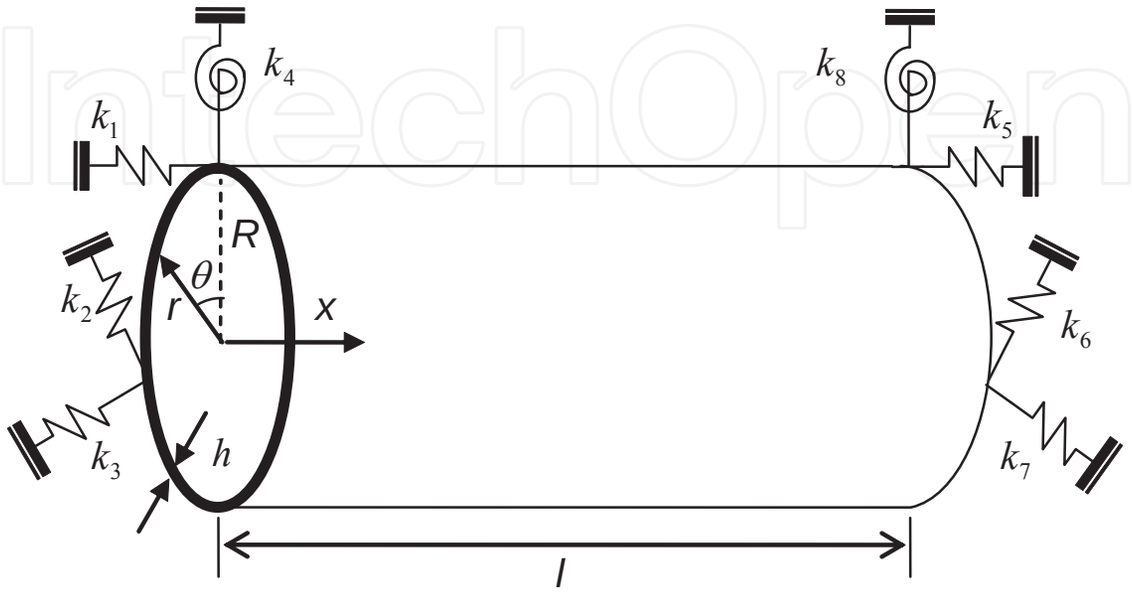

Figure 1. A circular cylindrical shell elastically restrained along all edges.

In terms of the shell displacements, the force and moment components can be expressed as

$$
\begin{aligned}
N_1 &= K\left(\frac{\partial u}{\partial x}+\sigma\frac{\partial v}{R\partial\theta}+\sigma\frac{w}{R}\right) && \text{(a)}\\
N_2 &= K\left(\frac{\partial v}{R\partial\theta}+\frac{w}{R}+\sigma\frac{\partial u}{\partial x}\right) && \text{(b)}\\
N_{12} &= K\frac{(1-\sigma)}{2}\left(\frac{\partial u}{R\partial\theta}+\frac{\partial v}{\partial x}\right) && \text{(c)}\\
M_1 &= -D\left(\frac{\partial^2 w}{\partial x^2}+\sigma\frac{\partial^2 w}{R^2\partial\theta^2}\right) && \text{(d)}\\
M_2 &= -D\left(\frac{\partial^2 w}{R^2\partial\theta^2}+\sigma\frac{\partial^2 w}{\partial x^2}\right) && \text{(e)}\\
M_{12} &= -D(1-\sigma)\frac{\partial^2 w}{R\partial x\partial\theta} && \text{(f)}\\
Q_1 &= \frac{\partial M_1}{\partial x}+\frac{\partial M_{12}}{R\partial\theta}=-D\left(\frac{\partial^3 w}{\partial x^3}+\frac{\partial^3 w}{R^2\partial x\partial\theta^2}\right) && \text{(g)}\\
Q_2 &= \frac{\partial M_2}{R\partial\theta}+\frac{\partial M_{12}}{\partial x}=-D\left(\frac{\partial^3 w}{R^3\partial\theta^3}+\frac{\partial^3 w}{R\partial x^2\partial\theta}\right) && \text{(h)}
\end{aligned}
\tag{2}
$$

where

$$\begin{aligned} K &= Eh/(1-\sigma^2), && \text{(a)} \\ D &= Eh^3/12(1-\sigma^2) && \text{(b)} \\ \kappa &= D/K = h^2/12 && \text{(c)} \end{aligned} \tag{3}$$

E and σ are respectively the Young's modulus and Poisson ratio of the material; M_1, M_2 and M_{12} are the bending and twisting moments.

The boundary conditions for an elastically restrained shell can specified as:

at x=0,

$$\begin{aligned} N_x - k_1 u &= 0 && \text{(a)} \\ N_{x\theta} - k_2 v &= 0 && \text{(b)} \\ Q_x + \frac{\partial M_{x\theta}}{R\partial\theta} - k_3 w &= 0 && \text{(c)} \\ M_x + k_4 \frac{\partial w}{\partial x} &= 0 && \text{(d)} \end{aligned} \tag{4}$$

at x=L,

$$\begin{aligned} N_x + k_5 u &= 0 && \text{(a)} \\ N_{x\theta} + k_6 v &= 0 && \text{(b)} \\ Q_x + \frac{\partial M_{x\theta}}{R\partial\theta} + k_7 w &= 0 && \text{(c)} \\ M_x - k_8 \frac{\partial w}{\partial x} &= 0 && \text{(d)} \end{aligned} \tag{5}$$

where k_1, k_2, …, k_8 are the stiffnesses for the restraining springs. The elastic supports represent a set of general boundary conditions, and all the classical boundary conditions can be considered as the special cases when the stiffness for each spring is equal to either zero or infinity.

The above equations are usually referred to as Donnell-Mushtari equations. Flügge's theory is also widely used to describe vibrations of shells. In terms of the shell displacements, the corresponding force and moment components are written as

http://dx.doi.org/10.5772/51816

$$
\begin{aligned}
N_1 &= K\left(\frac{\partial u}{\partial x}+\sigma\frac{\partial v}{R\partial\theta}\right)+K\sigma\frac{w}{R}-\frac{D}{R}\frac{\partial^2 w}{\partial x^2} && \text{(a)}\\
N_{12} &= \frac{1-\sigma}{2}K\left(\frac{\partial u}{R\partial\theta}+\frac{\partial v}{\partial x}\right)+\frac{D}{R}\frac{(1-\sigma)}{2}\left(\frac{\partial v}{R\partial x}-\frac{\partial^2 w}{R\partial\theta\partial x}\right) && \text{(b)}\\
N_2 &= K\left(\frac{\partial v}{R\partial\theta}+\frac{w}{R}+\sigma\frac{\partial u}{\partial x}\right)+\frac{D}{R}\left(\frac{\partial^2 w}{R^2\partial\theta^2}+\frac{w}{R^2}\right) && \text{(c)}\\
N_{21} &= \frac{1-\sigma}{2}K\left(\frac{\partial u}{R\partial\theta}+\frac{\partial v}{\partial x}\right)+\frac{D}{R}\frac{(1-\sigma)}{2}\left(\frac{\partial u}{R^2\partial\theta}+\frac{\partial^2 w}{R\partial\theta\partial x}\right) && \text{(d)}\\
M_1 &= -D\left(\frac{\partial^2 w}{\partial x^2}+\sigma\frac{\partial^2 w}{R^2\partial\theta^2}-\frac{\partial u}{R\partial x}-\sigma\frac{\partial v}{R^2\partial\theta}\right) && \text{(e)}\\
M_{12} &= -D(1-\sigma)\left(\frac{\partial^2 w}{R\partial\theta\partial x}-\frac{\partial v}{R\partial x}\right) && \text{(f)}\\
M_2 &= -D\left(\frac{w}{R^2}+\frac{\partial^2 w}{R^2\partial\theta^2}+\sigma\frac{\partial^2 w}{\partial x^2}\right) && \text{(g)}\\
M_{21} &= -D(1-\sigma)\left(\frac{\partial^2 w}{R\partial\theta\partial x}+\frac{1}{2}\frac{\partial u}{R^2\partial\theta}-\frac{1}{2}\frac{\partial v}{R\partial x}\right) && \text{(h)}\\
Q_1 &= -D\left(\frac{\partial^3 w}{\partial x^3}+\frac{1}{R^2}\frac{\partial^3 w}{\partial\theta^2\partial x}-\frac{\partial^2 u}{R\partial x^2}+\frac{1-\sigma}{2R^3}\frac{\partial^2 u}{\partial\theta^2}-\frac{1+\sigma}{2R^2}\frac{\partial v}{\partial x\partial\theta}\right) && \text{(i)}
\end{aligned}
\tag{6}
$$

A shell problem can be solved either exactly or approximately. An exact solution usually implies that both the governing equations and the boundary conditions are simultaneously satisfied exactly on a point-wise basis. Otherwise, a solution is considered approximate in which one or more of the governing equations and boundary conditions are enforced only in an approximate sense. Both solution strategies will be used below.

2.1. An approximate solution based on the Rayleigh-Ritz procedure

Approximate methods based on energy methods or the Rayleigh-Ritz procedures are widely used for the vibration analysis of shells with various boundary conditions and/or complicating factors. In such an approach, the displacement functions are usually expressed as

$$
\begin{aligned}
u(x,\theta) &= \sum_{m=0}^{\infty} a_m \varphi_u^m(x)\ \cos n\theta && \text{(a)}\\
v(x,\theta) &= \sum_{m=0}^{\infty} b_m \varphi_v^m(x)\ \sin n\theta && \text{(b)}\\
w(x,\theta) &= \sum_{m=0}^{\infty} c_m \varphi_w^m(x)\ \cos n\theta && \text{(c)}
\end{aligned}
\tag{7}
$$

where $\varphi_\alpha^m(x)$, $\alpha = u, v,$ and $w,$ are the characteristic functions for beams with *similar* boundary conditions. Although characteristic functions generally exist in the forms of trigonometric and hyperbolic functions, they also include some integration and frequency constants that have to be determined from boundary conditions. Consequently, each boundary condi-

tion basically calls for a special set of modal data. In the literature the modal parameters are well established for the simplest homogeneous boundary conditions. However, the determination of modal properties for the more complicated elastic boundary supports can become, at least, a tedious task since they have to be re-calculated each time when any of the stiffness values is changed. It should also be noted that calculating the modal properties will typically involve seeking the roots of a nonlinear transcendental equation, which mathematically requires an iterative root searching scheme and careful numerical implementations to ensure no missing data. To overcome this problem, a unified representation of the shell solutions will be adopted here in which the displacements, regardless of boundary conditions, will be invariably expressed as

$$u(x,\theta)=\left(\sum_{m=0}^{\infty} a_m \cos\lambda_m x + p_u(x)\right)\cos n\theta,\ (\lambda_m=\frac{m\pi}{L}) \quad \text{(a)}$$

$$v(x,\theta)=\left(\sum_{m=0}^{\infty} b_m \cos\lambda_m x + p_v(x)\right)\sin n\theta\ , \quad \text{(b)}$$

$$w(x,\theta)=\left(\sum_{m=0}^{\infty} c_m \cos\lambda_m x + p_w(x)\right)\cos n\theta \quad \text{(c)} \tag{8}$$

where $p_\alpha(x)$, $\alpha=u, v,$ and $w,$ denote three auxiliary polynomials which satisfy

$$\left.\frac{\partial p_u(x)}{\partial x}\right|_{x=0}=\left.\frac{\partial u(x,0)}{\partial x}\right|_{x=0}=\beta_1, \quad \text{(a)}$$

$$\left.\frac{\partial p_u(x)}{\partial x}\right|_{x=L}=\left.\frac{\partial u(x,0)}{\partial x}\right|_{x=L}=\beta_2 \quad \text{(b)}$$

$$\left.\frac{\partial p_v(x)}{\partial x}\right|_{x=0}=\left.\frac{\partial v(x,\pi/2)}{\partial x}\right|_{x=0}=\beta_3, \quad \text{(c)}$$

$$\left.\frac{\partial p_v(x)}{\partial x}\right|_{x=L}=\left.\frac{\partial v(x,\pi/2)}{\partial x}\right|_{x=L}=\beta_4, \quad \text{(d)}$$

$$\left.\frac{\partial p_w(x)}{\partial x}\right|_{x=0}=\left.\frac{\partial w(x,0)}{\partial x}\right|_{x=0}=\beta_5, \quad \text{(e)}$$

$$\left.\frac{\partial p_w(x)}{\partial x}\right|_{x=L}=\left.\frac{\partial w(x,0)}{\partial x}\right|_{x=L}=\beta_6, \quad \text{(f)}$$

$$\left.\frac{\partial^3 p_w(x)}{\partial x^3}\right|_{x=0}=\left.\frac{\partial^3 w(x,0)}{\partial x^3}\right|_{x=0}=\beta_7, \quad \text{(g)}$$

$$\left.\frac{\partial^3 p_w(x)}{\partial x^3}\right|_{x=L}=\left.\frac{\partial^3 w(x,0)}{\partial x^3}\right|_{x=L}=\beta_8 \quad \text{(h)} \tag{9}$$

It is clear from Eqs. (9) that these auxiliary polynomials are only dependent on the first and third derivatives β_i, (i=1,2,…,8) of the displacement solutions on the boundaries. In terms of boundary derivatives, the lowest-order polynomials can be explicitly expressed as [24, 25]

$$\begin{aligned} p_u(x) &= \zeta_1(x)\beta_1 + \zeta_2(x)\beta_2 && \text{(a)} \\ p_v(x) &= \zeta_1(x)\beta_3 + \zeta_2(x)\beta_4 && \text{(b)} \\ p_w(x) &= \zeta_1(x)\beta_5 + \zeta_2(x)\beta_6 + \zeta_3(x)\beta_7 + \zeta_4(x)\beta_8 && \text{(c)} \end{aligned} \tag{10}$$

where

$$\boldsymbol{\zeta}(x)^T = \begin{Bmatrix} \zeta_1(x) \\ \zeta_2(x) \\ \zeta_3(x) \\ \zeta_4(x) \end{Bmatrix} = \begin{Bmatrix} (6Lx - 2L^2 - 3x^2)/6L \\ (3x^2 - L^2)/6L \\ -(15x^4 - 60Lx^3 + 60L^2x^2 - 8L^4)/360L \\ (15x^4 - 30L^2x^2 + 7L^4)/360L \end{Bmatrix} \tag{11}$$

This alternative form of Fourier series recognizes the fact that the conventional Fourier series for a sufficiently smooth function $f(x)$ defined on a compact interval $[0, L]$ generally fails to converge at the end points. Introducing the auxiliary functions will ensure the cosine series in Eqs. (8) to converge uniformly and polynomially over the interval, including the end points. As a matter of fact, the polynomial subtraction techniques have been employed by mathematicians as a means to accelerate the convergence of the Fourier series expansion for an explicitly defined function [26-28].

The coefficients β_i represent the values of the first and third derivatives of the displacements at the boundaries, and are hence related to the unknown Fourier coefficients for the trigonometric terms. The relationships between the constants and the expansion coefficients can be derived either exactly or approximately.

In seeking an approximate solution based on an energy method, the solution is not required to explicitly satisfy the force or natural boundary conditions. Accordingly, the derivative parameters β_i in Eqs. (10) will be here determined from a simplified set of the boundary conditions, that is,

$$\begin{aligned} &\frac{\partial u}{\partial x} \mp \hat{k}_{1,5} u = 0 && \text{(a)} \\ &\frac{(1-\mu)}{2}\frac{\partial v}{\partial x} \mp \hat{k}_{2,6} v = 0 && \text{(b)} \\ &\kappa \frac{\partial^3 w}{\partial x^3} \pm \hat{k}_{3,7} w = 0 && \text{(c)} \\ &\kappa \frac{\partial^2 w}{\partial x^2} \mp \hat{k}_{4,8} \frac{\partial w}{\partial x} = 0 && \text{(d)} \end{aligned} \tag{12}$$

where

$$\hat{k}_i = k_i / K. \tag{13}$$

By substituting Eqs. (8) and (10) into (12), one will obtain

$$\begin{Bmatrix}\beta_1\\ \beta_2\end{Bmatrix} = \sum_{m=0}^{\infty} \mathbf{H}_u^{-1}\mathbf{Q}_u^m a_m \quad \text{(a)}$$

$$\begin{Bmatrix}\beta_3\\ \beta_4\end{Bmatrix} = \sum_{m=0}^{\infty} \mathbf{H}_v^{-1}\mathbf{Q}_v^m b_m \quad \text{(b)} \qquad (14)$$

$$\begin{Bmatrix}\beta_5 & \beta_6 & \beta_7 & \beta_8\end{Bmatrix}^T = \sum_{m=0}^{\infty} \mathbf{H}_w^{-1}\mathbf{Q}_w^m c_m \quad \text{(c)}$$

where

$$\mathbf{H}_u = \begin{bmatrix} \frac{\hat{k}_1 L}{3}+1 & \frac{\hat{k}_1 L}{6} \\ \frac{\hat{k}_5 L}{6} & \frac{\hat{k}_5 L}{3}+1 \end{bmatrix} \quad \text{(a)}$$

$$\mathbf{Q}_u^m = \begin{Bmatrix} \hat{k}_1 & (-1)^{m+1}\hat{k}_5 \end{Bmatrix}^{\mathrm{T}} \quad \text{(b)}$$

$$\mathbf{H}_v = \begin{bmatrix} \frac{\hat{k}_2 L}{3}+\frac{1-\mu}{2} & \frac{\hat{k}_2 L}{6} \\ \frac{\hat{k}_6 L}{6} & \frac{\hat{k}_6 L}{3}+\frac{1-\mu}{2} \end{bmatrix} \quad \text{(c)} \qquad (15)$$

$$\mathbf{Q}_v^m = \begin{Bmatrix} \hat{k}_2 & (-1)^{m+1}\hat{k}_6 \end{Bmatrix}^{\mathrm{T}} \quad \text{(d)}$$

$$\mathbf{H}_w = \begin{bmatrix} -\frac{\hat{k}_3 L}{3} & -\frac{\hat{k}_3 L}{6} & \frac{\hat{k}_3 L^3}{45}+\kappa & \frac{7\hat{k}_3 L^3}{360} \\ -\frac{\hat{k}_7 L}{6} & -\frac{\hat{k}_7 L}{3} & \frac{7\hat{k}_7 L^3}{360} & \frac{\hat{k}_7 L^3}{45}+\kappa \\ \hat{k}_4+\frac{\kappa}{L} & -\frac{\kappa}{L} & \frac{\kappa L}{3} & \frac{\kappa L}{6} \\ -\frac{\kappa}{L} & \hat{k}_8+\frac{\kappa}{L} & \frac{\kappa L}{6} & \frac{\kappa L}{3} \end{bmatrix} \quad \text{(e)}$$

and

$$\mathbf{Q}_w^m = \begin{Bmatrix} -\hat{k}_3 & (-1)^m\hat{k}_7 & -\kappa\lambda_m^2 & (-1)^m\kappa\lambda_m^2 \end{Bmatrix}^T \qquad (16)$$

In light of Eqs. (13), Eqs (8) can be reduced to Eqs. (7) with the axial functions being defined as

http://dx.doi.org/10.5772/51816

$$\varphi_\alpha^m(x) = \cos\lambda_m x + \boldsymbol{\zeta}(x)^T \bar{\mathbf{Q}}_\alpha^m, (\alpha = u, v, w) \tag{17}$$

where

$$\begin{aligned} \bar{\mathbf{Q}}_w^m &= \tilde{\mathbf{Q}}_w^m && \text{(a)} \\ \bar{\mathbf{Q}}_\alpha^m &= \begin{Bmatrix} \tilde{\mathbf{Q}}_\alpha^m \\ 0 \\ 0 \end{Bmatrix} && \text{(b)} \\ \tilde{\mathbf{Q}}_\alpha^m &= (\mathbf{H}_\alpha)^{-1}\mathbf{Q}_\alpha^m && \text{(c)} \end{aligned} \tag{18}$$

Since the boundary conditions are not exactly satisfied by the displacements such constructed, the Rayleigh-Ritz procedure will be employed to find a weak form of solution. The current solution is noticeably different from the conventional Rayleigh-Ritz solutions in that: a) the shell displacements are expressed in terms of three independent sets of axial functions, rather than a single (set of) beam function(s), b) the basis functions in each displacement expansion constitutes a complete set so that the convergence of the Rayleigh-Ritz solution is guaranteed mathematically, and c) it does not suffer from the well-known numerical instability problem related to the higher order beam functions or polynomials. More importantly, the current method is that it provides a unified solution to a wide variety of boundary conditions.

The potential energy consistent with the Donnell-Mushtari theory can be expressed from

$$\begin{aligned} V = \frac{K}{2}\int_0^L\int_0^{2\pi} \Bigg\{ & \left(\frac{\partial u}{\partial x} + \frac{\partial v}{R\partial\theta} + \frac{w}{R}\right)^2 - 2(1-\nu)\frac{\partial u}{\partial x}\left(\frac{\partial v}{R\partial\theta} + \frac{w}{R}\right) + \frac{(1-\nu)}{2}\left(\frac{\partial v}{\partial x} + \frac{\partial u}{R\partial\theta}\right)^2 + \\ & \kappa\left[\left(\frac{\partial^2 w}{\partial x^2} + \frac{\partial^2 w}{R^2\partial\theta^2}\right)^2 - 2(1-\nu)\left(\frac{\partial^2 w}{\partial x^2}\frac{\partial^2 w}{R^2\partial\theta^2} - \left(\frac{\partial^2 w}{R\partial x\partial\theta}\right)^2\right)\right]\Bigg\} R dx d\theta \\ & + 1/2\int_0^{2\pi} [k_1 u^2 + k_2 v^2 + k_3 w^2 + k_4\left(\partial w/\partial x\right)^2]_{x=0} R d\theta \\ & + 1/2\int_0^{2\pi} [k_5 u^2 + k_6 v^2 + k_7 w^2 + k_8\left(\partial w/\partial x\right)^2]_{x=L} R d\theta \end{aligned} \tag{19}$$

(a)

and the total kinetic energy is calculated from

$$T = \frac{1}{2}\int_0^L\int_0^{2\pi} \rho h\left[\left(\partial u/\partial t\right)^2 + \left(\partial v/\partial t\right)^2 + \left(\partial w/\partial t\right)^2\right] R dx d\theta \tag{b}$$

By minimizing the Lagrangian $L=V-T$ against all the unknown expansion coefficients, a final system of linear algebraic equations can be derived

$$\begin{bmatrix} \mathbf{\Lambda}^{ss} & \mathbf{\Lambda}^{s\theta} & \mathbf{\Lambda}^{sr} \\ \mathbf{\Lambda}^{s\theta\mathrm{T}} & \mathbf{\Lambda}^{\theta\theta} & \mathbf{\Lambda}^{\theta r} \\ \mathbf{\Lambda}^{sr\mathrm{T}} & \mathbf{\Lambda}^{\theta r\mathrm{T}} & \mathbf{\Lambda}^{rr} \end{bmatrix} \begin{Bmatrix} \bar{\mathbf{a}} \\ \bar{\mathbf{b}} \\ \bar{\mathbf{c}} \end{Bmatrix} - \omega^2 \begin{bmatrix} \mathbf{M}^{ss} & \mathbf{0} & \mathbf{0} \\ \mathbf{0} & \mathbf{M}^{\theta\theta} & \mathbf{0} \\ \mathbf{0} & \mathbf{0} & \mathbf{M}^{rr} \end{bmatrix} \begin{Bmatrix} \bar{\mathbf{a}} \\ \bar{\mathbf{b}} \\ \bar{\mathbf{c}} \end{Bmatrix} = 0 \tag{20}$$

where

$$\begin{aligned} \bar{\mathbf{a}} &= \left\{ a_{00}, a_{01}, \ldots, a_{mn}, \ldots \right\}^{\mathrm{T}}, \quad \text{(a)} \\ \bar{\mathbf{b}} &= \left\{ b_{01}, b_{02}, \ldots, b_{mn}, \ldots \right\}^{\mathrm{T}}, \quad \text{(b)} \\ \bar{\mathbf{c}} &= \left\{ c_{00}, c_{01}, \ldots, c_{mn}, \ldots \right\}^{\mathrm{T}}, \quad \text{(c)} \end{aligned} \tag{21}$$

$$\begin{aligned} \Lambda^{ss}_{mn,m'n'} &= \delta_{nn'}[I^{mm'}_{uu,11} + \frac{(1-\mu)n^2}{2R^2} I^{mm'}_{uu,00} + \frac{2}{L}\hat{k}_1 \varphi^m_u(0)\varphi^{m'}_u(0) + \frac{2}{L}\hat{k}_5 \varphi^m_u(L)\varphi^{m'}_u(L)] && \text{(a)} \\ \Lambda^{s\theta}_{mn,m'n'} &= \delta_{nn'}[\frac{\mu n}{R} I^{mm'}_{uv,10} - \frac{(1-\mu)n}{2R} I^{mm'}_{uv,01}] && \text{(b)} \\ \Lambda^{sr}_{mn,m'n'} &= \delta_{nn'} \frac{\mu}{R} I^{mm'}_{uw,10} && \text{(c)} \\ \Lambda^{\theta\theta}_{mn,m'n'} &= \delta_{nn'}[\frac{n^2}{R^2} I^{mm'}_{vv,00} + \frac{(1-\mu)}{2} I^{mm'}_{vv,11} + \frac{2}{L}\hat{k}_2 \varphi^m_v(0)\varphi^{m'}_v(0) + \frac{2}{L}\hat{k}_6 \varphi^m_v(L)\varphi^{m'}_v(L)] && \text{(d)} \\ \Lambda^{\theta r}_{mn,m'n'} &= \delta_{nn'} \frac{n}{R^2} I^{mm'}_{vw,00} && \text{(e)} \\ \Lambda^{\theta\theta}_{mn,m'n'} &= \delta_{nn'}\{\frac{1}{R^2} I^{mm'}_{ww,00} + \kappa[I^{mm'}_{ww,22} + \frac{n^4}{R^4} I^{mm'}_{ww,00} + 2(1-\mu)\frac{n^2}{R^2} I^{mm'}_{ww,11} \\ &\quad - \frac{\mu n^2}{R^2}(I^{mm'}_{ww,02} + I^{mm'}_{ww,20})] + \frac{2}{L}\hat{k}_3 \varphi^m_w(0)\varphi^{m'}_w(0) + \frac{2}{L}\hat{k}_7 \varphi^m_w(L)\varphi^{m'}_w(L) + && \text{(f)} \\ &\quad + \frac{2}{L}\hat{k}_4 \frac{\partial \varphi^m_w(0)}{\partial x}\frac{\partial \varphi^{m'}_w(0)}{\partial x} + \frac{2}{L}\hat{k}_8 \frac{\partial \varphi^m_w(L)}{\partial x}\frac{\partial \varphi^{m'}_w(L)}{\partial x}\} \end{aligned} \tag{22}$$

$$\begin{aligned} \mathbf{M}^{ss}_{mn,m'n'} &= \delta_{nn'} \rho h I^{mm'}_{uu,00} && \text{(a)} \\ \mathbf{M}^{\theta\theta}_{mn,m'n'} &= \delta_{nn'} \rho h I^{mm'}_{vv,00} && \text{(b)} \\ \mathbf{M}^{rr}_{mn,m'n'} &= \delta_{nn'} \rho h I^{mm'}_{ww,00} && \text{(c)} \end{aligned} \tag{23}$$

and

$$I^{mm'}_{\alpha\beta,pq} = 2/L \int_0^L \frac{\partial^p \phi^m_\alpha}{\partial x^p} \frac{\partial^q \phi^{m'}_\beta}{\partial x^q} dx \quad (\alpha, \beta = u, v, w) \tag{24}$$

The integrals in Eq. (23) can be calculated analytically; for instance

$$I^{mm'}_{\alpha\beta,00} = \frac{2}{L} \int_0^L \varphi_\alpha{}^m \varphi_\beta{}^{m'} \, dx$$

$$
\begin{aligned}
&= \frac{2}{L}\int_0^L (\cos\lambda_m x + \boldsymbol{\zeta}(x)^T \bar{\mathbf{Q}}_\alpha^m)(\cos\lambda_{m'} x + \boldsymbol{\zeta}(x)^T \bar{\mathbf{Q}}_\beta^{m'})\, dx \\
&= \frac{2}{L}\int_0^L (\cos\lambda_m x \cos\lambda_{m'} x + \cos\lambda_{m'} x \boldsymbol{\zeta}(x)^T \bar{\mathbf{Q}}_\alpha^m + \cos\lambda_m x \boldsymbol{\zeta}(x)^T \bar{\mathbf{Q}}_\beta^{m'} + \bar{\mathbf{Q}}_\alpha^{mT} \boldsymbol{\zeta}(x)\boldsymbol{\zeta}(x)^T \bar{\mathbf{Q}}_\beta^{m'})\, dx \\
&= \varepsilon_m \delta_{mm'} + S_\alpha^{m'm} + S_\beta^{mm'} + Z_{\alpha\beta}^{mm'}
\end{aligned}
\tag{25}
$$

where

$$
\begin{aligned}
\varepsilon_m &= (1+\delta_{m0}) && \text{(a)} \\
S_\alpha^{m'm} &= \mathbf{P}_c^{m'} \bar{\mathbf{Q}}_\alpha^m && \text{(b)} \\
Z_{\alpha\beta}^{mm'} &= \bar{\mathbf{Q}}_\alpha^{mT} \boldsymbol{\Xi} \bar{\mathbf{Q}}_\beta^{m'} && \text{(c)}
\end{aligned}
\tag{26}
$$

and

$$
\mathbf{P}_c^m = \frac{2}{L}\int_0^L \boldsymbol{\zeta}_w(x)^T \cos\lambda_m x\, dx \tag{27}
$$

$$
\begin{aligned}
&= \frac{2}{L}\begin{cases} \{\,0 \quad 0 \quad 0 \quad 0\,\}^T, & \text{for } m = 0 \\ \left\{\dfrac{-1}{\lambda_m^{\,2}} \quad \dfrac{(-1)^m}{\lambda_m^{\,2}} \quad \dfrac{1}{\lambda_m^{\,4}} \quad \dfrac{(-1)^{m+1}}{\lambda_m^{\,4}}\right\}^T, & \text{for } m \neq 0 \end{cases} && \text{(a)} \\
\boldsymbol{\Xi} &= 2/L\int_0^L \boldsymbol{\zeta}(x)^T \boldsymbol{\zeta}(x) dx = \begin{bmatrix} \dfrac{2L^2}{45} & & & \\ \dfrac{7L^2}{180} & \dfrac{2L^2}{45} & \textit{sym.} & \\ -\dfrac{4L^4}{945} & -\dfrac{31L^4}{7560} & \dfrac{2L^6}{4725} & \\ -\dfrac{31L^4}{7560} & -\dfrac{4L^4}{945} & \dfrac{127L^6}{302400} & \dfrac{2L^6}{4725} \end{bmatrix} && \text{(b)}
\end{aligned}
\tag{28}
$$

2.2. A strong form of solution based on Flügge's equations

As aforementioned, the displacement expressions in terms of beam functions cannot exactly satisfy the shell boundary conditions; instead they are made to satisfy the boundary conditions in a weak sense via the use of the Rayleigh-Ritz procedure. To overcome this problem, the displacement expressions, Eqs. (8), will now be generalized to

$$
\begin{aligned}
u(x,\theta) &= \sum_{n=0}^{\infty}\left(\sum_{m=0}^{\infty} A_{mn}\cos\lambda_m x + p_n^u(x)\right)\cos n\theta && \text{(a)} \\
v(x,\theta) &= \sum_{n=0}^{\infty}\left(\sum_{m=0}^{\infty} B_{mn}\cos\lambda_m x + p_n^v(x)\right)\sin n\theta && \text{(b)} \\
w(x,\theta) &= \sum_{n=0}^{\infty}\left(\sum_{m=0}^{\infty} C_{mn}\cos\lambda_m x + p_n^w(x)\right)\cos n\theta && \text{(c)}
\end{aligned}
\tag{29}
$$

which represent a 2-D version of the improved Fourier series expansions, Eqs. (8).

To demonstrate the flexibility in choosing the auxiliary functions $p_n^u(x)$, $p_n^v(x)$ and $p_n^w(x)$, an alternative set is used below:

$$\begin{aligned} p_n^u(x) &= \mathbf{\Lambda}_n^u \boldsymbol{\alpha}(x) \quad \text{(a)} \\ p_n^v(x) &= \mathbf{\Lambda}_n^v \boldsymbol{\alpha}(x) \quad \text{(b)} \\ p_n^w(x) &= \mathbf{\Lambda}_n^w \boldsymbol{\beta}(x) \quad \text{(c)} \end{aligned} \tag{30}$$

here $\Lambda_n^u = [a_n\ b_n]$, $\Lambda_n^v = [c_n\ d_n]$, $\Lambda_n^w = [e_n\ f_n\ g_n\ h_n]$ with a_n, b_n,..., g_n and h_n being the unknown coefficients to be determined; $\boldsymbol{\alpha}(x) = \{\alpha_1(x)\ \alpha_2(x)\}^{\mathrm{T}}$ and $\boldsymbol{\beta}(x) = \{\beta_1(x)\ \beta_2(x)\ \beta_3(x)\ \beta_4(x)\}^{\mathrm{T}}$ and with their elements being defined as

$$\begin{aligned} \alpha_1(x) &= x\left(\frac{x}{l} - 1\right)^2 \quad \text{(a)} \\ \alpha_2(x) &= \frac{x^2}{l}\left(\frac{x}{l} - 1\right) \quad \text{(b)} \end{aligned} \tag{31}$$

and

$$\begin{aligned} \beta_1(x) &= \frac{9l}{4\pi}\sin\left(\frac{\pi x}{2l}\right) - \frac{l}{12\pi}\sin\left(\frac{3\pi x}{2l}\right) && \text{(a)} \\ \beta_2(x) &= -\frac{9l}{4\pi}\cos\left(\frac{\pi x}{2l}\right) - \frac{l}{12\pi}\cos\left(\frac{3\pi x}{2l}\right) && \text{(b)} \\ \beta_3(x) &= \frac{l^3}{\pi^3}\sin\left(\frac{\pi x}{2l}\right) - \frac{l^3}{3\pi^3}\sin\left(\frac{3\pi x}{2l}\right) && \text{(c)} \\ \beta_4(x) &= -\frac{l^3}{\pi^3}\cos\left(\frac{\pi x}{2l}\right) - \frac{l^3}{3\pi^3}\cos\left(\frac{3\pi x}{2l}\right) && \text{(d)} \end{aligned} \tag{32}$$

In Eqs. (27), the sums of x-related terms are here understood as the series expansions in x-direction, rather than characteristic functions for a beam with "similar" boundary condition. This distinction is important in that the boundary conditions and governing differential equations can now be exactly satisfied on a point-wise basis; that is, the solution can be found in strong form, as described below.

Substituting Eqs. (6) and (27) into (4) and (5) will lead to

http://dx.doi.org/10.5772/51816

$$a_n - \left(\frac{7\sigma l}{3\pi R} + \frac{3\pi R\gamma}{4l}\right) f_n - \left(\frac{4\sigma l^3}{3\pi^3 R} + \frac{l\gamma R}{\pi}\right) h_n = \frac{k_1}{K}\sum_{m=0}^{\infty} A_{mn} - \frac{\sigma n}{R}\sum_{m=0}^{\infty} B_{mn} - \sum_{m=0}^{\infty}\left(\frac{\sigma}{R} + {\lambda_m}^2\gamma R\right) C_{mn} \quad \text{(a)}$$

$$\frac{1-\sigma}{2}(1+\gamma)c_n + \frac{(1-\sigma)\gamma n}{2} e_n = \frac{(1-\sigma)n}{2R}\sum_{m=0}^{\infty} A_{mn} + \frac{k_2}{K}\sum_{m=0}^{\infty} B_{mn} \quad \text{(b)}$$

$$-\frac{4}{lR}a_n - \frac{2}{lR}b_n + \frac{(3-\sigma)n}{2R^2}c_n + \frac{(2-\sigma)n^2}{R^2}e_n + \frac{7lk_3}{3\pi D}f_n - g_n + \frac{4l^3k_3}{3\pi^3 D}h_n = \sum_{m=0}^{\infty}\left(\frac{{\lambda_m}^2}{R} - \frac{(1-\sigma)n^2}{2R^3}\right)A_{mn} + \frac{k_3}{D}\sum_{m=0}^{\infty} C_{mn} \quad \text{(c)}$$

$$-\frac{1}{R}a_n + \left(\frac{3\pi}{4l} + \frac{7\nu l\,\mathrm{n}^2}{3\pi R^2}\right) f_n + \left(\frac{l}{\pi} + \frac{4\nu l^3 n^2}{3\pi^3 R^2}\right) h_n - \frac{k_4}{D} e_n = \frac{\sigma n}{R^2}\sum_{m=0}^{\infty} B_{mn} + \sum_{m=0}^{\infty}\left({\lambda_m}^2 + \frac{\sigma n^2}{R^2}\right) C_{mn} \quad \text{(d)} \quad (33)$$

$$-b_n - \left(\frac{3\pi\gamma R}{4l} + \frac{7\sigma l}{3\pi R}\right) e_n - \left(\frac{l\gamma R}{\pi} + \frac{4\sigma l^3}{3\pi^3 R}\right) g_n = \frac{k_5}{K}\sum_{m=0}^{\infty}\cos(m\pi)A_{mn} + \frac{n\sigma}{R}\sum_{m=0}^{\infty}\cos(m\pi)B_{mn} + \sum_{m=0}^{\infty}\left(\frac{\sigma}{R} + {\lambda_m}^2\gamma R\right)\cos(m\pi)C_{mn} \quad \text{(e)}$$

$$-\frac{1-\sigma}{2}(1+\gamma)d_n - \frac{(1-\sigma)n\gamma}{2} f_n = -\frac{(1-\sigma)n}{2R}\sum_{m=0}^{\infty}\cos(m\pi)A_{mn} + \frac{k_6}{K}\sum_{m=0}^{\infty}\cos(m\pi)B_{mn} \quad \text{(f)}$$

$$-\frac{2}{lR}a_n - \frac{4}{lR}b_n - \frac{(3-\sigma)n}{2R^2}d_n - \frac{7lk_7}{3\pi D}e_n - \frac{(2-\sigma)n^2}{R^2}f_n - \frac{4l^3k_7}{3\pi^3 D}g_n + h_n = -\sum_{m=0}^{\infty}\left(\frac{\cos(m\pi){\lambda_m}^2}{R} - \frac{(1-\sigma)\cos(m\pi)n^2}{2R^3}\right)A_{mn} + \frac{k_7}{D}\sum_{m=0}^{\infty}\cos(m\pi)C_{mn} \quad \text{(g)}$$

$$\frac{1}{R}b_n + \left(\frac{3\pi}{4l} + \frac{7\sigma l\,\mathrm{n}^2}{3\pi R^2}\right) e_n - \frac{k_8}{D} f_n + \left(\frac{l}{\pi} + \frac{4\sigma l^3\,\mathrm{n}^2}{3\pi^3 R^2}\right) g_n = -\frac{\sigma n}{R^2}\sum_{m=0}^{\infty}\cos(m\pi)B_{mn} - \sum_{m=0}^{\infty}\left({\lambda_m}^2 + \frac{\sigma n^2}{R^2}\right)\cos(m\pi)C_{mn} \quad \text{(h)}$$

Equations (31) represent a set of constraint conditions between the unknown (boundary) constants, a_n, b_n,..., g_n and h_n, and the Fourier expansion coefficients A_{mn}, B_{mn}, and C_{mn} (m, n = 0, 1, 2,...). The constraint equations (31a-h) can be rewritten more concisely, in matrix form, as

$$\mathbf{Ly} = \mathbf{Sx} \quad (34)$$

The elements of the coefficient matrices can be readily derived from Eqs. (31); for example, Eq. (31a) implies

$$
\begin{aligned}
&\left\{\mathbf{L}_{31}\right\}_{n,n'} = \delta_{nn'} && \text{(a)}\\
&\left\{\mathbf{L}_{36}\right\}_{n,n'} = -\left(\frac{7\sigma l}{3\pi R} + \frac{3\pi\gamma R}{4l}\right)\delta_{nn'} && \text{(b)}\\
&\left\{\mathbf{L}_{38}\right\}_{n,n'} = -\left(\frac{4\sigma l^3}{3\pi^3 R} + \frac{l\gamma R}{\pi}\right)\delta_{nn'} && \text{(c)}\\
&\left\{\mathbf{L}_{32}\right\}_{n,n'} = \left\{\mathbf{L}_{33}\right\}_{n,n'} = \left\{\mathbf{L}_{34}\right\}_{n,n'} = \left\{\mathbf{L}_{35}\right\}_{n,n'} = \left\{\mathbf{L}_{37}\right\}_{n,n'} = 0 && \text{(d)}\\
&\left\{\mathbf{S}_{11}\right\}_{mn,n'} = k_1\delta_{nn'} / K && \text{(e)}\\
&\left\{\mathbf{S}_{12}\right\}_{mn,n'} = -\sigma n\delta_{nn'} / R && \text{(f)}\\
&\left\{\mathbf{S}_{13}\right\}_{mn,n'} = -\delta_{nn'}\left(\frac{\sigma}{R} + \frac{m^2\pi^2\gamma R}{l^2}\right) && \text{(g)}
\end{aligned}
\qquad (35)
$$

Other sub-matrices can be similarly obtained from the remaining equations in Eqs. (31).

In actual numerical calculations, all the series expansions will have to be truncated to m=M and n=N. Thus there is a total number of (M+1)(3N+2)+8N+6 unknown expansion coefficients in the displacement functions. Since Eq. (33) represents a set of 8N+6 equations, additional (M+1)(3N+2) equations are needed to be able to solve for all the unknown coefficients. Accordingly, we will turn to the governing differential equations.

In Flügge's theory, the equations of motion are given as

$$
\begin{aligned}
&\frac{\partial N_1}{\partial x} + \frac{\partial N_{21}}{R\partial\theta} = \rho h\frac{\partial^2 u}{\partial t^2} && \text{(a)}\\
&\frac{\partial N_{12}}{\partial x} + \frac{\partial N_2}{R\partial\theta} + \left(\frac{\partial M_2}{R^2\partial\theta} + \frac{\partial M_{12}}{R\partial x}\right) = \rho h\frac{\partial^2 v}{\partial t^2} && \text{(b)}\\
&\frac{\partial^2 M_1}{\partial x^2} + \frac{\partial^2 M_{12}}{R\partial x\partial\theta} + \frac{\partial^2 M_{21}}{R\partial x\partial\theta} + \frac{\partial^2 M_2}{R^2\partial\theta^2} - \frac{N_2}{R} = \rho h\frac{\partial^2 w}{\partial t^2} && \text{(c)}
\end{aligned}
\qquad (36)
$$

Substituting Eqs. (6) and (37) into Eqs. (34) results in

http://dx.doi.org/10.5772/51816

$$
\begin{aligned}
&\sum_{m=0}^{\infty}\sum_{n=0}^{\infty}\left(-{\lambda_m}^2-\frac{(1-\sigma)(1+\gamma)n^2}{2R^2}\right)\cos\lambda_m x A_{mn}+\sum_{n=0}^{\infty}\mathbf{\Lambda}_n^u\left(\boldsymbol{\alpha}''(x)-\frac{(1-\sigma)(1+\gamma)n^2}{2R^2}\right)\\
&+\frac{(1+\sigma)}{2R}\left(-\sum_{m=0}^{\infty}\sum_{n=0}^{\infty}\lambda_m n\sin\lambda_m x B_{mn}+\sum_{n=0}^{\infty}n\mathbf{\Lambda}_n^v\boldsymbol{\alpha}'(x)\right)\\
&-\sum_{m=0}^{\infty}\sum_{n=0}^{\infty}\left(\frac{\sigma}{R}\lambda_m+\gamma R{\lambda_m}^3-\frac{(1-\sigma)\gamma n^2}{2R}\lambda_m\right)\sin\lambda_m x C_{mn} \qquad \text{(a)}\\
&+\sum_{n=0}^{\infty}\mathbf{\Lambda}_n^{w\mathrm{T}}\left(\frac{\sigma}{R}\boldsymbol{\beta}'(x)-\gamma R\boldsymbol{\beta}'''(x)-\frac{(1-\sigma)\gamma n^2}{2R}\boldsymbol{\beta}'(x)\right)\\
&+\frac{\omega^2\rho h}{K}\left(\sum_{m=0}^{\infty}\sum_{n=0}^{\infty}\cos\lambda_m x A_{mn}+\sum_{n=0}^{\infty}\mathbf{\Lambda}_n^u\boldsymbol{\alpha}(x)\right)=0\\
&+\frac{(1+\sigma)}{2R}\left(\sum_{m=0}^{\infty}\sum_{n=0}^{\infty}\lambda_m n\sin\lambda_m x A_{mn}-\sum_{n=0}^{\infty}n\mathbf{\Lambda}_n^u\boldsymbol{\alpha}'(x)\right)\\
&-\sum_{m=0}^{\infty}\sum_{n=0}^{\infty}\left(\frac{n^2}{R^2}+\frac{(1-\sigma)(1+3\gamma)}{2}{\lambda_m}^2\right)\cos\lambda_m x B_{mn}\\
&-\sum_{n=0}^{\infty}\mathbf{\Lambda}_n^{v\,\mathrm{T}}\left(\frac{n^2}{R^2}\boldsymbol{\alpha}(x)-\frac{(1-\sigma)(1+3\gamma)}{2}\boldsymbol{\alpha}''(x)\right) \qquad \text{(b)}\\
&-\sum_{m=0}^{\infty}\sum_{n=0}^{\infty}\left(\frac{n}{R^2}+\frac{(3-\sigma)\gamma n}{2}{\lambda_m}^2\right)\cos\lambda_m x C_{mn}\\
&-\sum_{n=0}^{\infty}\mathbf{\Lambda}_n^{w\mathrm{T}}\left(\frac{n}{R^2}\boldsymbol{\beta}(x)-\frac{(3-\sigma)\gamma n}{2}\boldsymbol{\beta}''(x)\right)\\
&+\frac{\omega^2\rho h}{K}\left(\sum_{m=0}^{\infty}\sum_{n=0}^{\infty}\cos\lambda_m x B_{mn}+\sum_{n=0}^{\infty}\mathbf{\Lambda}_n^v\boldsymbol{\alpha}(x)\right)=0\\
&-\sum_{m=0}^{\infty}\sum_{n=0}^{\infty}\left(\frac{\sigma}{R}-\frac{(1-\sigma)\gamma n^2}{2R}+\gamma R{\lambda_m}^2\right)\lambda_m\sin\lambda_m x A_{mn}\\
&+\sum_{n=0}^{\infty}\mathbf{\Lambda}_n^{u\,\mathrm{T}}\left(\frac{\sigma}{R}\boldsymbol{\alpha}'(x)-\frac{(1-\sigma)\gamma n^2}{2R}\boldsymbol{\alpha}'(x)-\gamma R\boldsymbol{\alpha}'''(x)\right)\\
&+\sum_{m=0}^{\infty}\sum_{n=0}^{\infty}\left(\frac{n}{R^2}+\frac{(3-\sigma)\gamma n}{2}{\lambda_m}^2\right)\cos\lambda_m x B_{mn}\\
&+\sum_{n=0}^{\infty}\mathbf{\Lambda}_n^{u\,\mathrm{T}}\left(\frac{n}{R^2}\boldsymbol{\alpha}(x)-\frac{(3-\sigma)\gamma n}{2}\boldsymbol{\alpha}''(x)\right) \qquad \text{(c)}\\
&+\sum_{m=0}^{\infty}\sum_{n=0}^{\infty}\left(\frac{1+\gamma(n^2+1)^2}{R^2}+R^2\gamma{\lambda_m}^4+2\gamma n^2{\lambda_m}^2\right)\cos\lambda_m x C_{mn}\\
&+\sum_{n=0}^{\infty}\mathbf{\Lambda}_n^{w\mathrm{T}}\left(\frac{1+\gamma(n^2+1)^2}{R^2}\boldsymbol{\beta}(x)-2\gamma n^2\boldsymbol{\beta}''(x)+\gamma R^2\boldsymbol{\beta}''''(x)\right)\\
&-\frac{\omega^2\rho h}{K}\left(\sum_{m=0}^{\infty}\sum_{n=0}^{\infty}\cos\lambda_m x C_{mn}+\sum_{n=0}^{\infty}\mathbf{\Lambda}_n^w\boldsymbol{\beta}(x)\right)=0
\end{aligned}
\tag{37}
$$

By expanding all non-cosine terms into Fourier cosine series and comparing the like terms, the following matrix equation can be obtained

$$\mathbf{Ex} + \mathbf{Fy} - \frac{\rho h \omega^2}{K}(\mathbf{Px} + \mathbf{Qy}) = 0. \tag{38}$$

where E, F, P and Q are coefficient matrices whose elements are given as:

$$\{\mathbf{E}_{11}\}_{mn,m'n'} = -\left(\lambda_m{}^2 + \frac{(1-\sigma)(1+\gamma)n^2}{2R^2}\right)\delta_{mm'}\delta_{nn'} \tag{a}$$

$$\{\mathbf{E}_{12}\}_{mn,m'n'} = -\frac{(1+\sigma)m'n\pi}{2lR}\chi_m^{m'}\delta_{mm'}\delta_{nn'} \tag{b}$$

$$\{\mathbf{E}_{13}\}_{mn,m'n'} = -\left(\frac{\sigma m'\pi}{lR} + \gamma\left(R\lambda_{m'}{}^3 - \frac{(1-\sigma)m'n^2\pi}{2lR}\right)\right)\chi_m^{m'}\delta_{mm'}\delta_{nn'} \tag{c}$$

$$\{\mathbf{E}_{21}\}_{mn,m'n'} = \frac{(1+\sigma)m'n\pi}{2lR}\chi_m^{m'}\delta_{mm'}\delta_{nn'} \tag{d}$$

$$\{\mathbf{E}_{22}\}_{mn,m'n'} = -\left(\frac{n^2}{R^2} + \frac{(1-\nu)(1+3\gamma)\lambda_m{}^2}{2}\right)\delta_{mm'}\delta_{nn'} \tag{e}$$

$$\{\mathbf{E}_{23}\}_{mn,m'n'} = -\left(\frac{n}{R^2} + \frac{(3-\nu)\gamma n\lambda_m{}^2}{2}\right)\delta_{mm'}\delta_{nn'} \tag{f}$$

$$\{\mathbf{E}_{31}\}_{mn,m'n'} = \left(-\frac{\nu\lambda_{m'}}{R} + \gamma\left(\frac{(1-\sigma)\lambda_{m'}n^2}{2R} - R\lambda_{m'}{}^3\right)\right)\chi_m^{m'}\delta_{mm'}\delta_{nn'} \tag{g}$$

$$\{\mathbf{E}_{32}\}_{mn,m'n'} = \left(\frac{n}{R^2} + \frac{(3-\sigma)\lambda_m{}^2 n\gamma}{2}\right)\delta_{mm'}\delta_{nn'} \tag{h}$$

$$\{\mathbf{E}_{33}\}_{mn,m'n'} = \left(\frac{1}{R^2} + \gamma\left(\left(R\lambda_m + \frac{n^2-1}{R}\right)^2 + 2\lambda_m\right)\right)\delta_{mm'}\delta_{nn'} \tag{i}$$

(39)

http://dx.doi.org/10.5772/51816

$$\left\{\mathbf{F}_{11-a}\right\}_{mn,n'}=\left(\psi_{1m}-\frac{(1-\sigma)(1+\gamma)n^2}{2R^2}\phi_{1m}\right)\delta_{nn'} \quad \text{(a)}$$

$$\left\{\mathbf{F}_{11-b}\right\}_{mn,n'}=\left(\psi_{2m}-\frac{(1-\sigma)(1+\gamma)n^2}{2R^2}\phi_{1m}\right)\delta_{nn'} \quad \text{(b)}$$

$$\left\{\mathbf{F}_{12-c}\right\}_{mn,n'}=\frac{(1+\sigma)n}{2R}\varphi_{1m}\delta_{nn'} \quad \text{(c)}$$

$$\left\{\mathbf{F}_{12-d}\right\}_{mn,n'}=\frac{(1+\sigma)n}{2R}\varphi_{2m}\delta_{nn'} \quad \text{(d)}$$

$$\left\{\mathbf{F}_{13-e}\right\}_{mn,n'}=\left(\left(\frac{9\sigma}{8R}+\gamma\left(\frac{9R\pi^2}{32l^2}-\frac{9(1-\sigma)n^2}{16R}\right)\right)\kappa_{2m}-\left(\frac{\sigma}{8R}+\gamma\left(\frac{9R\pi^2}{32l^2}-\frac{(1-\sigma)n^2}{16R}\right)\right)\kappa_{4m}\right)\delta_{nn'} \quad \text{(e)}$$

$$\left\{\mathbf{F}_{13-f}\right\}_{mn,n'}=\left(\left(\frac{9\sigma}{8R}+\gamma\left(\frac{9R\pi^2}{32l^2}-\frac{9(1-\sigma)n^2}{16R}\right)\right)\kappa_{1m}+\left(\frac{\sigma}{8R}+\gamma\left(\frac{9R\pi^2}{32l^2}-\frac{(1-\sigma)n^2}{16R}\right)\right)\kappa_{3m}\right)\delta_{nn'} \quad \text{(f)}$$

$$\left\{\mathbf{F}_{13-g}\right\}_{mn,n'}=\left(\left(\frac{\sigma l^2}{2\pi^2R}+\gamma\left(\frac{R}{8}-\frac{(1-\sigma)l^2n^2}{4\pi^2R}\right)\right)\kappa_{2m}-\left(\frac{\sigma l^2}{2\pi^2R}+\gamma\left(\frac{9R}{8}-\frac{(1-\sigma)l^2n^2}{4\pi^2R}\right)\right)\kappa_{4m}\right)\delta_{nn'} \quad \text{(g)}$$

$$\left\{\mathbf{F}_{13-h}\right\}_{mn,n'}=\left(\left(\frac{\sigma l^2}{2\pi^2R}+\gamma\left(\frac{R}{8}-\frac{(1-\sigma)l^2n^2}{4\pi^2R}\right)\right)\kappa_{1m}+\left(\frac{\sigma l^2}{2\pi^2R}+\gamma\left(\frac{9R}{8}-\frac{(1-\sigma)l^2n^2}{4\pi^2R}\right)\right)\kappa_{3m}\right)\delta_{nn'} \quad \text{(h)}$$

$$\left\{\mathbf{F}_{21-a}\right\}_{mn,n'}=-\frac{(1+\sigma)n}{2R}\varphi_{1m}\delta_{nn'} \quad \text{(i)}$$

$$\left\{\mathbf{F}_{21-b}\right\}_{mn,n'}=-\frac{(1+\sigma)n}{2R}\varphi_{2m}\delta_{nn'} \quad \text{(j)}$$

$$\left\{\mathbf{F}_{22-c}\right\}_{mn,n'}=-\left(\frac{n^2}{R^2}\phi_{1m}-\frac{(1-\sigma)(1+3\gamma)}{2}\psi_{1m}\right)\delta_{nn'} \quad \text{(k)}$$

$$\left\{\mathbf{F}_{22-d}\right\}_{mn,n'}=-\left(\frac{n^2}{R^2}\phi_{2m}-\frac{(1-\sigma)(1+3\gamma)}{2}\psi_{2m}\right)\delta_{nn'} \quad \text{(l)}$$

$$\left\{\mathbf{F}_{23-e}\right\}_{mn,n'}=-\left(\left(\frac{9nl}{4\pi R^2}+\frac{9\pi(3-\sigma)n\gamma}{32l}\right)\kappa_{1m}-\left(\frac{nl}{12\pi R^2}+\frac{3\pi(3-\sigma)n\gamma}{32l}\right)\kappa_{3m}\right)\delta_{nn'} \quad \text{(m)}$$

$$\left\{\mathbf{F}_{23-f}\right\}_{mn,n'}=\left(\left(\frac{9nl}{4\pi R^2}+\frac{9\pi(3-\sigma)n\gamma}{32l}\right)\kappa_{2m}+\left(\frac{nl}{12\pi R^2}+\frac{3\pi(3-\sigma)n\gamma}{32l}\right)\kappa_{4m}\right)\delta_{nn'} \quad \text{(n)} \qquad (40)$$

$$\left\{\mathbf{F}_{23-g}\right\}_{mn,n'}=-\left(\left(\frac{nl^3}{\pi^3R^2}+\frac{(3-\sigma)nl}{8\pi}\right)\kappa_{1m}-\left(\frac{nl^3}{3\pi^3R^2}+\frac{3(3-\sigma)nl\gamma}{8\pi}\right)\kappa_{3m}\right)\delta_{nn'} \quad \text{(o)}$$

$$\left\{\mathbf{F}_{23-h}\right\}_{mn,n'}=\left(\left(\frac{nl^3}{\pi^3R^2}+\frac{(3-\sigma)nl}{8\pi}\right)\kappa_{2m}+\left(\frac{nl^3}{3\pi^3R^2}+\frac{3(3-\sigma)nl\gamma}{8\pi}\right)\kappa_{4m}\right)\delta_{nn'} \quad \text{(p)}$$

$$\left\{\mathbf{F}_{31-a}\right\}_{mn,n'}=\left(\left(\frac{\sigma}{R}-\frac{(1-\sigma)\gamma n^2}{2R}\right)\varphi_{1m}-\frac{6R\gamma}{l^2}\delta_{m0}\right)\delta_{nn'} \quad \text{(o)}$$

$$\left\{\mathbf{F}_{31-b}\right\}_{mn,n'}=\left(\left(\frac{\sigma}{R}-\frac{(1-\sigma)\gamma n^2}{2R}\right)\varphi_{2m}-\frac{6R\gamma}{l^2}\delta_{m0}\right)\delta_{nn'} \quad \text{(r)}$$

$$\left\{\mathbf{F}_{32-c}\right\}_{mn,n'}=\left(\frac{n}{R^2}\phi_{1m}-\frac{(3-\sigma)n\gamma}{2}\psi_{1m}\right)\delta_{nn'} \quad \text{(s)}$$

$$\left\{\mathbf{F}_{32-d}\right\}_{mn,n'}=\left(\frac{n}{R^2}\phi_{21m}-\frac{(3-\sigma)n\gamma}{2}\psi_{2m}\right)\delta_{nn'} \quad \text{(t)}$$

$$\left\{\mathbf{F}_{33-e}\right\}_{mn,n'}=\left(\frac{9l}{4\pi}\left(\frac{1}{R^2}+\gamma\left(\left(\frac{R\pi^2}{4l^2}+\frac{n^2-1}{R}\right)^2+\frac{\pi^2}{2l^2}\right)\right)\kappa_{1m}-\frac{l}{3\pi}\left(\frac{1}{4R^2}+\gamma\left(\left(\frac{9R\pi^2}{8l^2}+\frac{n^2-1}{2R}\right)^2+\frac{9\pi^2}{8l^2}\right)\right)\kappa_{3m}\right)\delta_{nn'} \quad \text{(u)}$$

$$\left\{\mathbf{F}_{33-f}\right\}_{mn,n'}=-\left(\frac{9l}{4\pi}\left(\frac{1}{R^2}+\gamma\left(\left(\frac{R\pi^2}{4l^2}+\frac{n^2-1}{R}\right)^2+\frac{\pi^2}{2l^2}\right)\right)\kappa_{2m}-\frac{l}{3\pi}\left(\frac{1}{4R^2}+\gamma\left(\left(\frac{9R\pi^2}{8l^2}+\frac{n^2-1}{2R}\right)^2+\frac{9\pi^2}{8l^2}\right)\right)\kappa_{4m}\right)\delta_{nn'} \quad \text{(v)}$$

$$\left\{\mathbf{F}_{33-g}\right\}_{mn,n'}=\left(\frac{l}{\pi}\left(\frac{l^2}{\pi^2R^2}+\gamma\left(\left(\frac{R\pi}{4l}+\frac{\left(n^2-1\right)l}{\pi R}\right)^2-\frac{1}{2}\right)\right)\kappa_{1m}-\frac{l}{3\pi}\left(\frac{l^2}{\pi^2R^2}+\gamma\left(\left(\frac{9R\pi}{4l}+\frac{\left(n^2-1\right)l}{\pi R}\right)^2-\frac{9}{2}\right)\right)\kappa_{3m}\right)\delta_{nn'} \quad \text{(w)}$$

$$\left\{\mathbf{F}_{33-h}\right\}_{mn,n'}=-\left(\frac{l}{\pi}\left(\frac{l^2}{\pi^2R^2}+\gamma\left(\left(\frac{R\pi}{4l}+\frac{\left(n^2-1\right)l}{\pi R}\right)^2-\frac{1}{2}\right)\right)\kappa_{2m}-\frac{l}{3\pi}\left(\frac{l^2}{\pi^2R^2}+\gamma\left(\left(\frac{9R\pi}{4l}+\frac{\left(n^2-1\right)l}{\pi R}\right)^2-\frac{9}{2}\right)\right)\kappa_{4m}\right)\delta_{nn'} \quad \text{(x)}$$

$$
\begin{aligned}
&\left\{\mathbf{P}_{11}\right\}_{mn,m'n'}=\left\{\mathbf{P}_{22}\right\}_{mn,m'n'}=-\left\{\mathbf{P}_{33}\right\}_{mn,m'n'}=-\delta_{mm'}\delta_{nn'} && \text{(a)}\\
&\left\{\mathbf{Q}_{11-a}\right\}_{mn,n'}=\left\{\mathbf{Q}_{22-c}\right\}_{mn,n'}=-\phi_{1m}\delta_{nn'} && \text{(b)}\\
&\left\{\mathbf{Q}_{11-b}\right\}_{mn,n'}=\left\{\mathbf{Q}_{22-d}\right\}_{mn,n'}=-\phi_{2m}\delta_{nn'} && \text{(c)}\\
&\left\{\mathbf{Q}_{33-e}\right\}_{mn,n'}=\frac{l}{4\pi}\left(9\kappa_{1m}-\frac{\kappa_{3m}}{3}\right)\delta_{nn'} && \text{(d)}\\
&\left\{\mathbf{Q}_{33-f}\right\}_{mn,n'}=-\frac{l}{4\pi}\left(9\kappa_{2m}+\frac{\kappa_{4m}}{3}\right)\delta_{nn'} && \text{(e)}\\
&\left\{\mathbf{Q}_{33-g}\right\}_{mn,n'}=\frac{l^3}{\pi^3}\left(\kappa_{1m}-\frac{\kappa_{3m}}{3}\right)\delta_{nn'} && \text{(f)}\\
&\left\{\mathbf{Q}_{33-h}\right\}_{mn,n'}=-\frac{l^3}{\pi^3}\left(\kappa_{2m}+\frac{\kappa_{4m}}{3}\right)\delta_{nn'} && \text{(g)}
\end{aligned}
\tag{41}
$$

The symbols κ_{1m}, κ_{2m}, κ_{3m}, κ_{4m}, ϕ_{1m}, ϕ_{2m}, φ_{1m}, φ_{2m}, ψ_{1m}, ψ_{2m}, and χ_m^i in the above equations are defined as

$$
\begin{aligned}
&\sin\left(\frac{\pi}{2l}x\right)=\sum_{m=0}^{\infty}\kappa_{1m}\cos\lambda_m x; && \kappa_{1m}=\begin{cases}\dfrac{2}{\pi} & m=0,\\ \dfrac{4}{(1-4m^2)\pi} & m\neq 0,\end{cases} && \text{(a,b)}\\
&\cos\left(\frac{\pi}{2l}x\right)=\sum_{m=0}^{\infty}\kappa_{2m}\cos\lambda_m x; && \kappa_{2m}=\begin{cases}\dfrac{2}{\pi} & m=0,\\ \dfrac{4(-1)^m}{(1-4m^2)\pi} & m\neq 0,\end{cases} && \text{(c,d)}\\
&\sin\left(\frac{3\pi}{2l}x\right)=\sum_{m=0}^{\infty}\kappa_{3m}\cos\lambda_m x; && \kappa_{3m}=\begin{cases}\dfrac{2}{3\pi} & m=0,\\ \dfrac{12}{(9-4m^2)\pi} & m\neq 0,\end{cases} && \text{(e,f)}\\
&\cos\left(\frac{3\pi}{2l}x\right)=\sum_{m=0}^{\infty}\kappa_{4m}\cos\lambda_m x; && \kappa_{4m}=\begin{cases}-\dfrac{2}{3\pi} & m=0,\\ \dfrac{12(-1)^{m+1}}{(9-4m^2)\pi} & m\neq 0,\end{cases} && \text{(g, h)}\\
&\alpha_1(x)=\sum_{m=0}^{\infty}\phi_{1m}\cos\lambda_m x; && \phi_{1m}=\begin{cases}\dfrac{l}{12} & m=0,\\ -\dfrac{2l\left(m^2\pi^2-6+6(-1)^m\right)}{m^4\pi^4} & m\neq 0,\end{cases} && \text{(i,j)}\\
&\alpha_2(x)=\sum_{m=0}^{\infty}\phi_{2m}\cos\lambda_m x; && \phi_{2m}=\begin{cases}-\dfrac{l}{12} & m=0,\\ \dfrac{2l\left(m^2\pi^2(-1)^m+6-6(-1)^m\right)}{m^4\pi^4} & m\neq 0,\end{cases} && \text{(k, l)}\\
&\alpha_1'(x)=\sum_{m=0}^{\infty}\varphi_{1m}\cos\lambda_m x; && \varphi_{1m}=\begin{cases}0 & m=0,\\ \dfrac{4\left(2+(-1)^m\right)}{m^2\pi^2} & m\neq 0,\end{cases} && \text{(m,n)}\\
&\alpha_2'(x)=\sum_{m=0}^{\infty}\varphi_{2m}\cos\lambda_m x; && \varphi_{2m}=\begin{cases}0 & m=0,\\ \dfrac{4\left(1+2(-1)^m\right)}{m^2\pi^2} & m\neq 0,\end{cases} && \text{(o,p)}\\
&\alpha_1''(x)=\sum_{m=0}^{\infty}\psi_{1m}\cos\lambda_m x; && \psi_{1m}=\begin{cases}-\dfrac{1}{l} & m=0,\\ \dfrac{12\left(-1+(-1)^m\right)}{lm^2\pi^2} & m\neq 0,\end{cases} && \text{(q,r)}\\
&\alpha_2''(x)=\sum_{m=0}^{\infty}\psi_{2m}\cos\lambda_m x; && \psi_{2m}=\begin{cases}\dfrac{1}{l} & m=0,\\ \dfrac{12\left(-1+(-1)^m\right)}{lm^2\pi^2} & m\neq 0,\end{cases} && \text{(s, t)}\\
&\sin\lambda_m x=\sum_{i}^{\infty}\chi_i^m\cos\lambda_i x=\sin\lambda_i x=\sum_{m}^{\infty}\chi_m^i\cos\lambda_m x; && \chi_m^i=\begin{cases}0 & i=0,\\ \begin{cases}\dfrac{1-(-1)^i}{i\pi} & m=0,\\ \dfrac{2i\left[(-1)^{m+i}-1\right]}{(m^2-i^2)\pi} & m\neq 0,\end{cases} & i\neq 0.\end{cases} && \text{(u, v)}
\end{aligned}
\tag{42}
$$

http://dx.doi.org/10.5772/51816

All the unmentioned elements in matrices P and Q are identically equal to zero.

Equations (32) and (36) can be combined into

$$\left(\mathbf{K} - \frac{\rho h \omega^2}{K}\mathbf{M}\right)\mathbf{x} = 0, \tag{43}$$

where $K = E + F L^{-1} S$ and $M = P + Q L^{-1} S$.

The final system of equations, Eq. (19) or (41), represents a standard characteristic equation for a matrix eigen-problem from which all the eigenvalues and eigenvectors can be readily calculated. It should be mentioned that the elements in each eigenvector are actually the expansion coefficients for the corresponding mode; its "physical" mode shape can be directly obtained from Eqs. (7) or (27).

In the above discussions, the stiffness distribution for each restraining spring is assumed to be axisymmetric or uniform along the circumference. However, this restriction is not necessary. For non-uniform elastic boundary restraints, the displacement expansions, Eq. (27), shall be used, and any and all of stiffness constants can be simply understood as varying with spatial angle θ. For simplicity, we can universally expand these functions into standard cosine series and modify Eq. (31) accordingly to reflect this complicating factor.

3. Results and discussion

Several numerical examples will be given below to verify the two solution strategies described earlier.

3.1. Results about the approximate Rayleigh-Ritz solution

We first consider a familiar simply-supported cylindrical shell. The simply supported boundary condition, $N_x = M_x = v = w = 0$at each end, can be considered as a special case when $k_{2,6} = k_{3,7} = \infty$ and $k_{1,5} = k_{4,8} = 0$ (in actual calculations, infinity is represented by a sufficiently large number). To examine the convergence of the solution, Table 1 shows the frequency parameters, $\Omega = \omega R\sqrt{\rho(1-\sigma^2)/E}$, calculated using different numbers of terms in the series expansions. It is seen that the solution converges nicely with only a small number of terms. In the following calculations, the expansions in axial direction will be simply truncated to M=15. Given in Table 2 are the frequencies parameters for some lower-order modes. Exact solution is available for the simply supported case and the results are also shown there for comparison. An excellent agreement is observed between these two sets of results. Although the simply supported boundary condition represents the simplest case in shell analysis, this problem is not trivial in testing the reliability and sophistication of the current solution method. From numerical analysis standpoint, it may actually represent a quite challenging case because of the extreme stiffness values involved. The non-trivialness can also been seen

mathematically from the fact that the simple sine function (in the axial direction) in the exact solution is actually expanded as a cosine series expansion in the current solution.

Number of terms used in the series	$\Omega=\omega R\sqrt{\rho(1-\sigma^2)/E}$				
	n=0	*n=1*	*n=2*	*n=3*	*n=4*
M=5	0.464652	0.257389	0.127132	0.143329	0.234823
M=7	0.464649	0.257386	0.127129	0.143327	0.234822
M=9	0.464648	0.257385	0.127128	0.143327	0.234822
M=10	0.464648	0.257385	0.127128	0.143327	0.234822

Table 1. Frequency parameters, $\Omega=\omega R\sqrt{\rho(1-\sigma^2)/E}$, obtained using different numbers of terms in the displacement expansions.

Mode	$\Omega=\omega R\sqrt{\rho(1-\sigma^2)/E}$				
	n=0	*n=1*	*n=2*	*n=3*	*n=4*
m=1, Current	0.464648	0.257385	0.127128	0.143327	0.234822
Exact	0.464648	0.257385	0.127128	0.143327	0.234822
m=2, Current	0.928907	0.574179	0.337652	0.248813	0.285620
Exact	0.928907	0.574176	0.337649	0.248810	0.285619
m=3, Current	0.948172	0.764375	0.532951	0.399893	0.383688
Exact	0.948172	0.764355	0.532923	0.399865	0.383667

Table 2. Frequency parameters, $\Omega=\omega R\sqrt{\rho(1-\sigma^2)/E}$, for a simply-supported shell; L=4R, h/R=0.05 and μ=0.3.

Next, consider a cylindrical shell clamped at each end, that is,$u=v=w=\partial w/\partial x=0$. The clamped-clamped boundary condition is a case when the stiffnesses of the restraining springs all become infinitely large. The related shell and material parameters are as follows: L=0.502 m, R=0.0635 m, h=0.00163 m, E=2.1×10^{11}, μ=0.28, and ρ=7800. Listed in Table 3 are some of the lowest natural frequencies for this clamped-clamped shell. The reference results given there are calculated from

$$\Omega^6 - A_2\Omega^4 + A_1\Omega^2 - A_0 = 0 \tag{44}$$

where$\Omega=\omega R\sqrt{\rho(1-\sigma^2)/E}$, and the coefficients A_0, A_1 and A_2 are the functions of the modal indices, shell parameters, and the boundary conditions [27]. Equation (42) can be derived from the Rayleigh-Ritz procedure by adopting the beam characteristic functions as the axial functions for all three displacement components. A noticeable difference between these two sets of results may be attributed to the fact that: a) Eq. (42) given in ref. [29] is based on the Flügge shell theory, rather than the Donnell-Mushtari theory, and b) Eq. (42) uses only a sin-

gle beam characteristic function in contrast to the three complete sets (of basis functions) in the current method.

Mode	Current m=1	Eq. (42)	Current m=2	Eq. (42)
n=1	1886.74	2035.05	3854.75	4302.05
2	934.220	971.531	2039.66	2189.59
3	982.265	990.339	1454.80	1500.07
4	1598.55	1600.90	1769.54	1782.28
5	2484.78	2486.49	2572.31	2578.07

Table 3. The natural frequencies in Hz for a clamped-clamped shell; L=0.502 m, R=0.0635 m, h=0.00163 m, E=2.1E+11, μ=0.28, ρ=7800 kg/m^3.

Mode	*n=2*	*n=3*	*n=4*	*n=5*	*n=6*	*n=7*
Translation:						
current	0.00413	0.00986	0.01792	0.02830	0.04099	0.05599
(2.130) [22]	0.00310	0.00876	0.01680	0.02717	0.03986	0.05487
FEA	0.00310	0.00876	0.01679	0.02714	0.03980	0.05475
Rotation:						
Current	0.01907	0.01676	0.02068	0.02995	0.04220	0.05713
(2.132) [22]	0.00343	0.00924	0.01734	0.02774	0.04045	0.05546
FEA	0.00343	0.00923	0.01731	0.02769	0.04037	0.05533
m=1:						
Current	0.24075	0.13190	0.08343	0.06292	0.05906	0.06606
FEA	0.23810	0.12836	0.07938	0.05893	0.05555	0.06332

Table 4. Frequency parameters, $\Omega = \omega R\sqrt{\rho(1-\sigma^2)/E}$, for a free-free shell; R=0.5 m, L=4R, h=0.002R, and μ=0.28.

Another classical example involves a completely free shell. Vibration of a free-free shell is of particular interest as manifested in the debate between two legendary figures, Rayleigh and Love, about the validity of the inextensional theory of shells. The lower-order modes are typically related to the rigid-body motions in the axial direction. Theoretically, the H_w matrix given in Eqs. (14) will become non-invertible for a completely free shell. However, this numerical irregularity can be easily avoided by letting one of the bending-related springs have a very small stiffness, such as,$\hat{k}_4$=10^{-6}. Table 4 shows a comparison of the frequency parameters calculated using different techniques. While the results obtained from the current technique agree reasonably well with the other two reference sets, perhaps within the variance of different shell theories, the frequency parameters for the two lower order modes with rigid-body rotation (n=2 and 3) are clearly inaccurate which probably indicates that the inability of exactly satisfying the shell boundary conditions by the "beam functions" tends

to have more serious consequence in such a case. Amazingly enough, the inextensional theory works very well in predicting the frequency parameters for the "rigid-body" modes (those with rigid-body motions in the axial direction). It is also seen that the frequency parameters of the rigid-body modes increases monotonically with the circumferential modal index n.

After it has been adequately illustrated how the classical boundary conditions can be easily and universally dealt with by simply changing the stiffness values of the restraining springs, we will direct our attention to shells with elastic end restraints. For the purpose of comparison, the problems previously studied in ref. [20] will be considered here. It was observed in that study that the tangential stiffness had the greatest effect on the natural frequency of the cylinder supported at both ends while the axial boundary stiffness had the greatest influence on the natural frequency of the cylinder supported at one end. It was also determined that natural frequencies varied rapidly with the boundary flexibility when the non-dimensionalized stiffness is between 10^{-2} and 10^{2}.

The frequency parameters for the "clamped"-free shell are shown in Table 5 for the reduced axial stiffness $\hat{k}_1 L\ (1-\mu^2)=1$ (corresponding to $k_u^*=1$ in ref. [20]). It is seen that the current results are slightly larger than those taken from ref. [20]. The possible reasons include: 1) the difference in shell theories (the Flügge theory, rather than the Donnell-Mushtari, was used there), and 2) different Poisson ratios may have been used in the calculations.

Mode	*n=0*	*n=1*	*n=2*	*n=3*	*n=4*	*n=5*
m=1	0.9752	0.514686	0.32866 (0.315*)	0.361036	0.532604 (0.498)	0.782661
m=2	1.22044	1.12788	1.08573	1.10467	1.16021	1.432

Note: the numbers in parentheses are taken from ref. [20]

Table 5. Frequency parameters, $\Omega=\omega R\sqrt{\rho(1-\sigma^2)/E}$, for a "clamped"-free shell; R=0.00625 m, $L=R$, $h=0.1R$, μ=0.28, and $\hat{k}_1 L\ (1-\mu^2)=1$.

Although all eight sets of springs can be independently specified here, for simplicity we will only consider a simple configuration: a cantilevered shell with an elastic support being attached to its free (right) end in the radial direction. Listed in Table 6 are the four lowest natural frequencies for several different stiffness values. Obviously, the cases for $\hat{k}_7=0$ and ∞ represent the clamped-free and clamped-simply supported boundary conditions, respectively.

The mode shapes for the three intermediate stiffness values are plotted in Figs. 2-4. It is seen that the modal parameters can be significantly modified by the stiffness of the restraining springs. The four modes in Fig. 2 for $\hat{k}_7=0.01\ \mathrm{m}^{-1}$ closely resemble their counterparts in the clamped-free case, even though the natural frequencies have been modified noticeably. While all the first four natural frequencies happen to increase, more or less, with the spring stiffness, the modal sequences are not necessarily the same. For example, when the spring

http://dx.doi.org/10.5772/51816

stiffness $\hat{k}_7$ is increased from 0.01 to 0.1 m^{-1}, the third natural frequency goes from 886.66 to 926.17 Hz. However, this frequency drift may not necessarily reflect the direct effect of the stiffness change on the (original) third mode. It is evident from Figs. 2 and 3 that the third and fourth modes are actually switched in these two cases: the original third mode now becomes the fourth at 1200.88 Hz. It is also interesting to note that while stiffening the elastic support $\hat{k}_7$ (from 0.01 to 0.1 m^{-1}) has significantly raised the natural frequencies for the first two modes, the fourth mode is adversely affected: its frequency has actually dropped from 1023.61 to 926.17 Hz (see Figs. 2 and 3). A similar trend is also observed between the fourth mode for $\hat{k}_7$=0.1 m^{-1} and the second mode for $\hat{k}_7$=1 m^{-1}, as shown in Figs. 3 and 4.

Mode	$\hat{k}_7=0$	$\hat{k}_7=0.01$	$\hat{k}_7=0.1$	$\hat{k}_7=1$	$\hat{k}_7=10^{10}$
1	404.108	451.242	627.345	729.593	742.920
2	487.598	513.222	679.082	935.745	936.719
3	865.603	886.656	926.173	1084.91,	1269.58
4	1003.38	1023.61	1200.88	1319.99, ,	1333.37

Table 6. Natural frequencies in Hz for a clamped-elastically supported shell; L=0.502 m, R=0.0635 m, h=0.00163 m, E=2.1E+11, μ=0.28, ρ=7800 kg/m^3;$\hat{k}_5=\hat{k}_6=\hat{k}_8=0$.

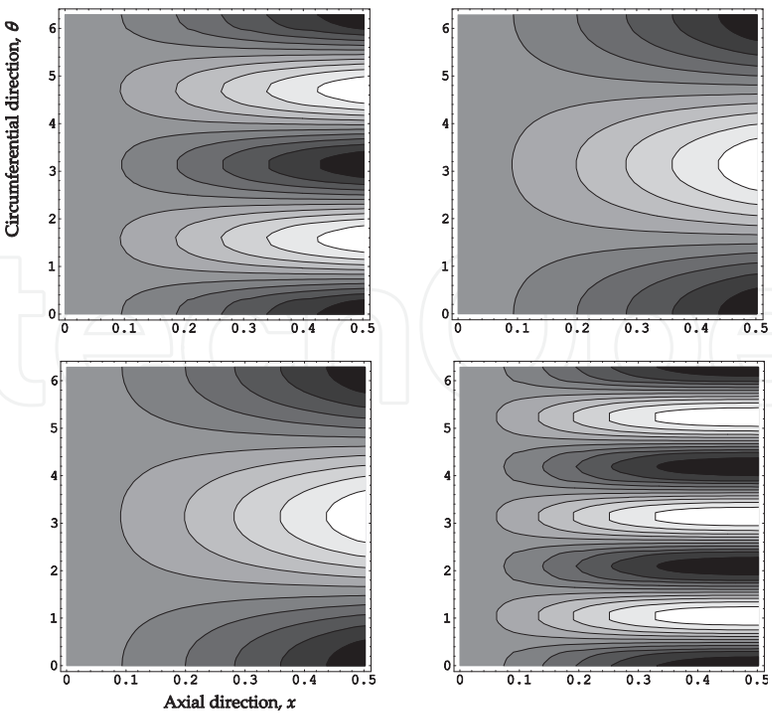

Figure 2. First four modes for the clamped-elastically supported shell; $\hat{k}_7$=0.01 $m^{-1}$and$\hat{k}_5=\hat{k}_6=\hat{k}_8=0$.

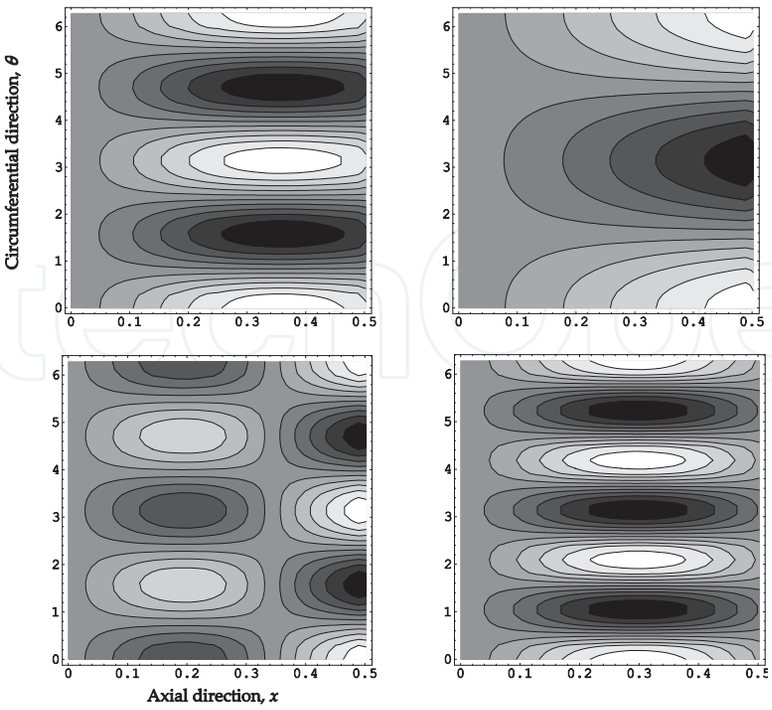

Figure 3. First four modes for the clamped-elastically supported shell; $\hat{k}_7 = 0.1\ \mathrm{m}^{-1}$ and $\hat{k}_5 = \hat{k}_6 = \hat{k}_8 = 0$.

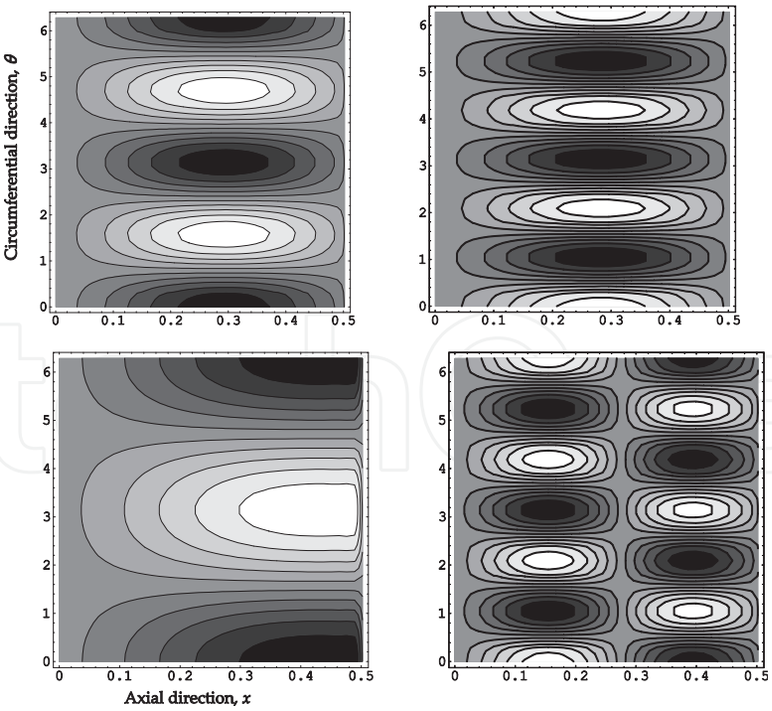

Figure 4. First four modes for the clamped-elastically supported shell; $\hat{k}_7 = 1\ \mathrm{m}^{-1}$ and $\hat{k}_5 = \hat{k}_6 = \hat{k}_8 = 0$.

http://dx.doi.org/10.5772/51816

3.2. An exact solution based on the Flügge's equations

To validate the exact solution method, the simply supported shell is considered again. Given in Table 7 are the calculated natural frequency parameters $\Omega = \omega R\sqrt{\rho(1-\sigma^2)/E}$. The current results agree well with the exact solutions based on Flügge's theory [30], solutions based on beam functions [31] and three-dimensional linear elasticity solutions [30].

h/R	n	$\Omega = \omega R\sqrt{\rho(1-\sigma^2)/E}$			
		Ref. [30][a]	Ref. [31]	Ref. [30][b]	Present
0.05	0	0.0929586	0.0929682	0.0929296	0.0929590
	1	0.0161065	0.0161029	0.0161063	0.0161064
	2	0.0393038	0.0392710	0.0392332	0.0393035
	3	0.1098527	0.1098113	0.1094770	0.1098468
	4	0.2103446	0.2102770	0.2090080	0.2103419
0.002	0	0.0929296	0.0929298	0.0929296	0.0929299
	1	0.0161011	0.0161011	0.0161011	0.0161023
	2	0.0054532	0.0054530	0.0054524	0.0054547
	3	0.0050419	0.0050415	0.0050372	0.0050427
	4	0.0085341	0.0085338	0.0085341	0.0085344

[a] Exact solutions based on Flügge's theory.

[b] Three-dimensional linear elasticity solutions.

Table 7. Comparison of values of the natural frequency parameter $\Omega = \omega R\sqrt{\rho(1-\sigma^2)/E}$ for a circular cylindrical shell with simply supported boundary conditions, $m = 1$, $R/l = 0.05$, $\sigma = 0.3$.

n	m = 1			m = 2		
	FEM	present	difference (%)	FEM	present	difference (%)
0	3229.8	3230.3	0.015%	5131.4	5131.1	0.006%
1	2478.6	2479.3	0.028%	4830.4	4830.6	0.004%
2	269.20	269.30	0.037%	276.62	278.58	0.704%
3	761.25	761.01	0.032%	770.99	771.62	0.082%
4	1459.2	1458.6	0.041%	1469.6	1469.3	0.020%
5	2359.4	2358.6	0.034%	2369.9	2369.0	0.038%

Table 8. Comparison of values of the natural frequency for a circular cylindrical shell with free-free boundary conditions, L=0.502 m, R=0.0635 m, h=0.00163 m, σ =0.28, E=2.1E+11 N/m^3, ρ=7800 kg/m^3.

The current solution method is also compared with the finite element model (ANSYS) for shells under free-free boundary condition. In the FEM model, the shell surface is divided into 8000 elements with 8080 nodes. The calculated natural frequencies are compared in Tables 8. An excellent agreement is observed between these two solution methods.

In most techniques, such as the wave approach, the beam functions for the analogous boundary conditions are often used to determine the axial modal wavenumbers. While such an approach is exact for a simply supported shell, and perhaps acceptable for slender thin shells, it may become problematic for shorter shells due to the increased coupling of the radial and two in-plane displacements. To illustrate this point, we consider relatively shorter and thicker shell (l=8R and R =39h). The calculated natural frequencies are compared in Table 9 for a clamped-clamped shell. It is seen that while the current and FEM results are in good agreement, the frequencies obtained from the wave approach (based on the use of beam functions) are significantly higher, especially for the lower order modes.

n	m = 1			m = 2		
	FEM	Ref. [32]	present	FEM	Ref. [32]	Present
0	3229.8	4845.5	3230.3	5146.0	8075.8	5139.8
1	1882.8	2350.2	1880.9	3850.7	4775.6	3848.9
2	899.59	985.48	898.18	2017.8	2303.4	2014.1
3	896.97	919.01	896.56	1390.9	1479.2	1388.9
4	1501.9	1517.45	1501.6	1676.4	1714.0	1676.0
5	2386.1	2402.05	2386.0	2472.5	2501.8	2472.6

Table 9. Comparison of the natural frequencies for a circular cylindrical shell with clamped-clamped boundary conditions, L=0.502 m, R=0.0635 m, h=0.00163 m, σ=0.28, E=2.1E+11 N/m^3, ρ=7800 kg/m^3.

The exact solution method can be readily applied to shells with elastic boundary supports. Since the above examples are considered adequate in illustrating the reliability and accuracy of the current method, we will not elaborate further by presenting the results for elastically restrained shells. Instead, we will simply point out that the solution method based on Eqs. (27) is also valid for non-uniform or varying boundary restraint along the circumferential direction, which represents a significant advancement over many existing techniques.

4. Conclusion

An improved Fourier series solution method is described for vibration analysis of cylindrical shells with general elastic supports. This method can be easily and universally applied to a wide variety of boundary conditions including all the 136 classical homogeneous boundary conditions. The displacement functions are invariantly expressed as series expansions in terms of the complete set of trigonometric functions, which can mathematically ensure

http://dx.doi.org/10.5772/51816

the accuracy and convergence of the present solution. From practical point of view, the change of boundary conditions here is as simple as varying a typical shell or material parameter (e.g., thickness or mass density), and does not involve any solution algorithm and procedure modifications to adapt to different boundary conditions. In addition, the proposed method does not require pre-determining any secondary data such as modal parameters for an "analogous" beam, or modifying the implementation algorithms to avoid the numerical instabilities resulting from computer round-off errors. It should be mentioned that the current method can be readily extended to shells with arbitrary non-uniform elastic restraints. The accuracy and reliability of the current solutions have been demonstrated through numerical examples involving various boundary conditions.

Acknowledgments

The authors gratefully acknowledge the financial support from the National Natural Science Foundation of China (No. 50979018).

Author details

Tiejun Yang[1], Wen L. Li[2] and Lu Dai[1]

1 College of Power and Energy Engineering, Harbin Engineering University, Harbin, PR China

2 Department of Mechanical Engineering, Wayne State University, Detroit, USA

References

[1] Influence of boundary conditions on the modal characteristics of thin cylindrical shells,. AIAA Journal ; , 2-2150.

[2] Forsberg, K. Axisymmetric and beam-type vibrations of thin cylindrical shells,. AIAA Journal (1969). , 7-221.

[3] Warburton, G. B. Vibrations of thin circular cylindrical shell, J. Mech. Eng. Sci. (1965). , 7-399.

[4] Warburton, G. B., & Higgs, J. Natural frequencies of thin cantilever cylindrical shells. J. Sound Vib. (1970). , 11-335.

[5] Goldman, R. L. (1974). Mode shapes and frequencies of clamped-clamped cylindrical shells. *AIAA Journal*, 12-1755.

[6] Yu, Y. Y. Free vibrations of thin cylindrical shells having finite lengths with freely supported and clamped edges, J. Appl. Mech. (1955). , 22-547.

[7] Berglund, J. W., & Klosner, J. M. Interaction of a ring-reinforced shell and a fluid medium. J. Appl. Mech., (1968). , 35-139.

[8] De Silva, C. N., & Tersteeg, C. E. Axisymmetric vibrations of thin elastic shells. J. Acoust. Soc. Am. (1964). , 4-666.

[9] Smith, B. L., & Haft, E. E. (1968). Natural frequencies of clamped cylindrical shells,. *AIAA Journal*, 6-720.

[10] Li, X. A., new, approach., for, free., vibration, analysis., of, thin., circular, cylindrical., & shell, J. Sound Vib. (2006). , 296, 91-98.

[11] Wang, C., & Lai, J. C. S. (2000). Prediction of natural frequencies of finite length circular cylindrical shells. *Applied Acoustics*, 59-385.

[12] Zhang, X. M., Liu, G. R., & Lam, K. Y. Vibration analysis of thin cylindrical shells using wave propagation approach,. Journal of Sound and Vibration (2001). , 239(3), 397-403.

[13] Li, X. B. (2008). Study on free vibration analysis of circular cylindrical shells using wave propagation. *Journal of Sound and Vibration*, 311-667.

[14] Arnold, R. N., & Warburton, G. B. Flexural vibrations of the walls of thin cylindrical shells having freely supported ends. Proc. Roy. Soc., A (1949). , 197-238.

[15] Arnold, R. N., & Warburton, G. B. The flexural vibrations of thin cylinders. Proc. Inst. Mech. Engineers, A (1953). , 167, 62-80.

[16] Sharma, C. B., & Johns, D. J. Vibration characteristics of a clamped-free and clamped-ring-stiffened circular cylindrical shell, J. Sound Vib. 1971;. 14-459.

[17] Sharma, C. B., & Johns, D. J. Free vibration of cantilever circular cylindrical shells-a comparative study, J. Sound Vib. (1972). , 25-433.

[18] Sharma, C. B. Calculation of natural frequencies of fixed-free circular cylindrical shells. J. Sound Vib. (1974). , 35-55.

[19] Soedel, W. A., new, frequency., formula, for., closed, circular., cylindrical, shells., for, a., large, variety., of, boundary., & conditions, . J. Sound Vib. (1980). , 70-309.

[20] Loveday, P. W., & Rogers, C. A. Free vibration of elastically supported thin cylinders including gyroscopic effects,. J. Sound Vib, (1998). , 217, 547-562.

[21] Amabili, M., & Garziera, R. Vibrations of circular cylindrical shells with nonuniform constraints, elastic bed and added mass: part I: empty and fluid-filled shells. J. Fluids Struct, (2000). , 14, 669-690.

[22] Leissa A. W. Vibration of Shells, Acoustical Society of America; 1993.

[23] Qatu M.S. (2002). Recent research advances in the dynamic behavior of shells. part 2: homogeneous shells,. *Applied Mechanics Reviews*, 55, 415-434.

[24] Li, W. L. Free vibrations of beams with general boundary conditions. J. Sound Vib. (2000). , 237-709.

[25] Li, W. L. Vibration analysis of rectangular plates with general elastic boundary supports. J. Sound Vib. (2004). , 273-619.

[26] Lanczos, C. Discourse on Fourier series. Hafner, New York; (1966).

[27] Jones, W. B., & Hardy, G. Accelerating convergence of trigonometric approximations. Math. Comp. (1970). , 24-547.

[28] Baszenski, G., Delvos, J., Tasche, M. A., united, approach., to, accelerating., trigonometric, expansions., & Comput, . Math. Appl. (1995). , 30-33.

[29] Blevins, R. D. Formulas for Natural Frequency and Mode Shape. New York: Van Nostrand Reinhold Company; (1979).

[30] Khdeir, A. A., & Reddy, J. N. Influence of edge conditions on the modal characteristics of cross-ply laminted shells, Computers and Structures (1990). , 34-817.

[31] Lam, K. Y., & Loy, C. T. (1995). Effects of boundary conditions on frequencies of a multi-layered cylindrical shell. *Journal of Sound and Vibration*, 363-384.

[32] Zhang, X. M., Liu, G. R., & Lam, K. Y. Vibration analysis of thin cylindrical shells using wave propagation approach,. Journal of Sound and Vibration (2001). , 239(3), 397-403.

IntechOpen